Biomedicine & Pharmacotherapy 191 (2025) 118497

Contents lists available at ScienceDirect

Biomedicine & Pharmacotherapy

journal homepage: www.elsevier.com/locate/biopha

Empagliflozin reduces left ventricular mass increase and improves cardiomyocyte hypertrophy after 5/6 nephrectomy

Xin Chen [a,b,h], Christian T. Wohnhaas [c], Denis Delić [b,c], Nicolas Schommer [d,f], Daniel Duerschmied [d,e,f], Yaochen Cao [b,g], Zeyu Zhang [b,h], Christoph Reichetzeder [a], Mohamed M.S. Gaballa [b,i,j], Bernhard K. Krämer [b,e], Thomas Klein [k], Ben He [l], Linghong Shen [l], Berthold Hocher [b,m,n,*]

[a] Institute for Clinical Research and Systems Medicine, Health and Medical University, Potsdam, Germany
[b] Fifth Department of Medicine (Nephrology/Endocrinology/Rheumatology/Pneumology), University Medical Centre Mannheim, University of Heidelberg, Germany
[c] Translational Medicine & Clinical Pharmacology, Boehringer Ingelheim Pharma GmbH & Co. KG, Birkendorferstr.65, Biberach 88397, Germany
[d] Cardiology, Angiology, Haemostaseology, and Medical Intensive Care, Medical Centre Mannheim and Medical Faculty Mannheim, Heidelberg University, Germany
[e] European Center for AngioScience (ECAS), German Centre for Cardiovascular Research (DZHK) partner site Heidelberg/ Mannheim, and Centre for Cardiovascular Acute Medicine Mannheim (ZKAM), Medical Centre Mannheim and Medical Faculty Mannheim, Heidelberg University, Germany
[f] Helmholtz-Institute for Translational AngioCardioScience (HI-TAC) of the Max Delbrück Center for Molecular Medicine in the Helmholtz Association (MDC) at Heidelberg University, Germany
[g] Department of Nephrology, Charité - Universitätsmedizin Berlin, Campus Mitte, Berlin, Germany
[h] The First Clinical Medical College of Jinan University, The First Affiliated Hospital of Jinan University, Guangzhou, China
[i] Academy of Scientific Research and Technology (ASRT), Cairo 11516, Egypt
[j] Department of Pathology, Faculty of Veterinary Medicine, Benha University, PO Box 13736, Benha, Toukh, Egypt
[k] Department of Cardiometabolic Diseases Research, Boehringer Ingelheim Pharma GmbH & Co. KG, Birkendorfer Str. 65, Biberach 88397, Germany
[l] Department of Cardiology, Shanghai Chest Hospital, Shanghai Jiao Tong University School of Medicine, Shanghai, China
[m] Reproductive and Genetic Hospital of CITIC-Xiangya, Changsha, China
[n] IMD Institut für Medizinische Diagnostik Berlin-Potsdam GbR, Berlin, Germany

ARTICLE INFO

Keywords:
Empagliflozin
5/6 nephrectomy
Cardiomyocyte hypertrophy
Left ventricular mass

ABSTRACT

Left ventricular hypertrophy (LVH) is a common cardiac complication in patients with cardiorenal syndrome. Empagliflozin has demonstrated cardio-renal protective effects in clinical studies, potentially linked to reductions in left ventricular mass (LVM). Using a 5/6 nephrectomy rat model to induce cardiorenal syndrome, we administered two doses of Empagliflozin (3 mg/kg/day and 15 mg/kg/day) via gavage for 95 days, with Telmisartan as a positive control. Cardiac structure and function were assessed using echocardiography, histological analysis, and serum biomarkers. Single-nucleus RNA sequencing (snRNA-seq) and quantitative real-time polymerase chain reaction (qRT-PCR) were employed to investigate molecular mechanisms. The 5/6 nephrectomy

Abbreviation: 5/6Nx, 5/6 Nephrectomy; Angpt1, Angiopoietin 1; ARB, Angiotensin II Receptor Blocker; AWT, Anterior Wall Thickness; BMP2, Bone Morphogenetic Protein 2; BNP, B-type Natriuretic Peptide; BP, Blood Pressure; CAD, Coronary Artery Disease; CKD, Chronic Kidney Disease; CMRI, Cardiac Magnetic Resonance Imaging; DAPI, 4',6-Diamidino-2-Phenylindole; DEGs, Differentially Expressed Genes; EF, Ejection Fraction; ER, Endoplasmic Reticulum; ERK, Extracellular Signal-Regulated Kinase; ESRD, End-Stage Renal Disease; FDR, False Discovery Rate; Fhl2, Four and a Half LIM Domains 2; FS, Fractional Shortening; GO, Gene Ontology; HCM, Hypertrophic Cardiomyopathy; HFrEF, Heart Failure with Reduced Ejection Fraction; HPLC, High Performance Liquid Chromatography; IC, Immune Cell; INOS, Inducible Nitric Oxide Synthase; IVS, Interventricular Septum; IVSd, IVS in Diastole; IVSs, IVS in Systole; KEGG, Kyoto Encyclopedia of Genes and Genomes; LVEDd, Left Ventricular End-Diastolic Dimension; LVEDV, Left Ventricular End-Diastolic Volume; LVESd, Left Ventricular End-Systolic Dimension; LVESV, Left Ventricular End-Systolic Volume; LVM, Left Ventricular Mass; LVPW, Left Ventricular Posterior Wall; LVPWd, Left Ventricular Posterior Wall in Diastole; LVPWs, Left Ventricular Posterior Wall in Systole; LVH, Left Ventricular Hypertrophy; MAPK, Mitogen-Activated Protein Kinase; MAST, Model-based Analysis of Single-cell Transcriptomics; NFAT, Nuclear Factor of Activated T Cells; PBO, Placebo; PCs, Principal Components; PSmad, Phosphorylated SMAD; QRT-PCR, Quantitative Real-Time Polymerase Chain Reaction; SGLT2, Sodium-Glucose Cotransporter 2; SnRNA-seq, Single-Nuclei RNA Sequencing; SV, Stroke Volume; T2DM, Type 2 Diabetes Mellitus; TBE, Tribromoethanol; Tbx20, T-box Transcription Factor 20; UMAP, Uniform Manifold Approximation and Projection; UMI, Unique Molecular Identifier.

* Corresponding author at: Fifth Department of Medicine (Nephrology/Endocrinology/Rheumatology/Pneumology), University Medical Centre Mannheim, University of Heidelberg, Germany.
E-mail address: berthold.hocher@medma.uni-heidelberg.de (B. Hocher).

https://doi.org/10.1016/j.biopha.2025.118497
Received 12 June 2025; Received in revised form 13 August 2025; Accepted 23 August 2025
Available online 28 August 2025

increased serum creatinine, troponin T, LVM, ejection fraction, and cardiomyocyte diameter. Empagliflozin treatment significantly decreased LVM and cardiomyocyte hypertrophy, comparable to Telmisartan. snRNA-seq revealed no changes in major cardiac cell populations but identified differential expression of cardiomyocyte development genes, including *Fhl2*, *Tbx20*, and *Angpt1*. qRT-PCR data for Fhl2 and Tbx20 aligned with the snRNA-seq data, showing that Empagliflozin increased Fhl2 expression and decreased Tbx20 expression. Immunofluorescence showed increased myocardial infiltration of M2 macrophages, CD4 + T cells, and CD8 + T cells in Empagliflozin-treated rats, but there was no difference between the 5/6 nephrectomized rats and normal rats. In a non-diabetic cardiorenal syndrome model, Empagliflozin effectively attenuated left ventricular hypertrophy and cardiomyocyte enlargement. These effects appear mediated by the regulation of genes involved in cardiomyocyte development and myocardial remodeling (*Fhl2* and *Tbx20*), rather than cardiomyocyte proliferation. These findings highlight Empagliflozin's cardioprotective potential in cardiorenal syndrome and provide a foundation for further clinical exploration.

1. Introduction

Chronic kidney disease (CKD), especially end-stage renal disease (ESRD), significantly increases the risk of cardiovascular diseases, including myocardial hypertrophy, heart failure, and coronary artery disease (CAD) [1]. Left ventricular hypertrophy (LVH) is the most common cardiac structural abnormality in CKD patients, affecting up to 70 % of ESRD patients [2,3]. Multiple factors contribute to uremic cardiomyopathy, including hemodynamic overload, changes in mineral metabolism, insulin resistance, accumulation of circulating uremic toxins, increased endogenous cardiotonic steroids, oxidative stress, and chronic inflammation [3]. Furthermore, damage to the heart further accelerates the deterioration of the kidneys [4]. Exploring treatments that can benefit both the kidneys and the heart simultaneously has long been considered a key area of research in this field.

Empagliflozin, a sodium-glucose cotransporter 2 (SGLT2) inhibitor, is used in the treatment of type 2 diabetes (T2DM) to lower blood sugar. The main pharmacological action of empagliflozin is to inhibit SGLT2, which is located in the proximal renal tubule, thereby preventing more than 90 % of sodium and glucose from being reabsorbed in the renal tubules [5]. Notably, many large-scale controlled clinical trials have reported that SGLT2 inhibitors not only effectively lower blood glucose but also provide protective effects on the heart and kidneys in both diabetic and non-diabetic patients. The EMPA-KIDNEY trial [6], a clinical study involving 6609 CKD patients, showed that empagliflozin not only slowed the decline in glomerular filtration rate (GFR) but also reduced the incidence of kidney disease progression or death due to cardiovascular disease. Additionally, clinical trials, including the DAPA-CKD trial involving 4304 non-diabetic CKD patients [7] and the REG OUTCOME trial involving 7020 patients with T2DM [8], have further supported this finding. The EMPEROR-Reduced clinical trial [9] and the EMPEROR-Preserved clinical trial [10] studied over 3000 heart failure patients (regardless of whether they had diabetes) and showed that empagliflozin reduced the relative risk of cardiovascular death or hospitalization for heart failure in patients with an ejection fraction (EF) $\leq$ 40 % and EF $>$ 40 %. More importantly, a clinical trial focusing on nondiabetic HFrEF (heart failure with reduced ejection fraction), EMPA-TROPISM [11,12], not only analyzed cardiovascular mortality but also assessed cardiac structural and functional parameters. The study suggested that empagliflozin improved left ventricular mass (LVM) and left ventricular systolic function in heart failure patients, while also reducing myocardial interstitial fibrosis and inflammation markers. Subsequently, more clinical trials (DAPA-LVH trial [13]; EMPA-HEART CardioLink-6 [14]) indicated that SGLT2 inhibitors (empagliflozin/dapagliflozin) significantly reduced left ventricular mass (LV mass) in patients with T2DM or CAD. In the EMPA-HEART CardioLink-6 trial, the beneficial effect of empagliflozin on LVM was observed within the 6-month treatment period. This early separation of the Kaplan-Meier curves for cardiovascular death and heart failure hospitalization in the EMPA-REG OUTCOME trial aligns with these findings. Therefore, the study proposed that the improvement in LVM with empagliflozin might be a contributing factor to the favorable cardiovascular outcomes observed in the EMPA-REG OUTCOME trial. Given that changes in LVM are a key causal determinant of cardiovascular events and mortality, understanding how SGLT2 inhibitors affect myocardial structure and function is crucial. Accordingly, we are exploring the mechanisms in a classic nondiabetic CKD rat model (5/6 nephrectomy) to provide valuable therapeutic insights for patients with cardiorenal syndrome.

2. Materials and methods

2.1. Experimental animals and protocol

Animal experiments were approved by the Animal Care and Use Committee of Jinan University, Guangzhou, China (IACUC-20190830–02). All animal experiments complied with the ARRIVE guidelines and were conducted in accordance with the U.K. Animals (Scientific Procedures) Act, 1986 and associated guidelines, as well as the National Research Council's Guide for the Care and Use of Laboratory Animals.

Seven-week-old male Wistar rats were purchased from Vital River Laboratory Animal Technology Co., Ltd (Beijing). The rats were kept at a room temperature of 22–25°C, a humidity of 55 ± 5 %, a 12-hour light/dark cycle, and were fed standard rat chow and water. After a 7-day adaptation, the rats were randomly divided into five groups: sham operation + placebo (10 rats), 5/6 nephrectomy (Nx) + placebo (15 rats); 5/6Nx + telmisartan (5 mg/kg/day, 15 rats), 5/6Nx + 3 mg empagliflozin (3 mg/kg/day, 15 rats); 5/6Nx + 15 mg empagliflozin (15 mg/kg/day, 15 rats). The 5/6Nx procedure was performed under anaesthesia with 2,2,2-tribromomethanol (500 mg/kg intraperitoneal injection) as follows: unilateral nephrectomy of the right kidney (Uni-Nx) was performed on week 1 and bipolar nephrectomy of the left kidney on week 3. At the same time points, the Sham + PBO group received all operations except nephrectomy. Drug or vehicle treatment was administered by gavage from the first day after surgery until 24 h before euthanasia, for a period of 95 days. Empagliflozin was manufactured by Boehringer Ingelheim Pharma GmbH & Co. KG (Biberach an der Riss, Germany), and the dose was selected based on previous studies [15–17]. A 0.5 % w/v hydroxypropyl methylcellulose aqueous solution was used as a vehicle for empagliflozin. Rats in the control groups (Sham+PBO and 5/6Nx+PBO) were only given 0.5 % w/v hydroxypropyl methylcellulose solution by gavage. At the end of the study, the rats were examined by echocardiography (vevo 770TM-230, VisualSonics, Canada) in the parasternal long axis view and blood pressure was measured using the tail-cuff method (BP-2000 Blood Pressure Analysis System, model BP-2000-RP-4, Visitech Systems, USA). Twenty-four hours before the end of the study, urine was collected as follows: Rats were placed individually in metabolic cages and urine was collected for 24 h and the volume recorded. The urine was then centrifuged at 12,000 rpm for 10 min at 4°C and the resulting supernatant was stored at −80°C for further analysis. Due to disease and surgical losses, the final number of animals in each group was as follows: Sham + Placebo (7 rats), 5/6Nx + Placebo (9 rats), 5/6Nx + 3 mg Empagliflozin (9 rats),

5/6Nx + 15 mg Empagliflozin (11 rats), and 5/6Nx + Telmisartan (7 rats). Rats were euthanised in week 18, and blood and hearts were collected. Pharmacological treatment was stopped 24 h before euthanasia. Blood samples were collected from the abdominal aorta under anaesthesia with 2,2,2-tribromomethanol (500 mg/kg i.p.). The collected blood samples were centrifuged at 3000 rpm for 10 min at 4°C, and the supernatant was stored at −80°C for further analysis. The heart (ventricles and atria) was weighed and cut into two parts: the upper part of the heart was fixed in 4 % formaldehyde solution for further histological analysis, and the remaining part was stored at −80°C for later analysis. Tribromoethanol (TBE) was used for both terminal and short survival procedures, as it was the only approved anesthetic available at our institution during the study. Its use was IACUC-approved and limited to brief interventions with appropriate post-procedure care. All personnel were well trained in its preparation and administration, and solutions were freshly prepared and properly stored. Under these conditions, TBE was a justified and suitable choice for our experimental needs.

2.2. Serum and urine analysis

Serum creatinine and serum troponin T concentrations were measured using an ~~automatic~~ automated biochemical analyser (Siemens biochemical analyser and its Leadman reagents, Siemens, Germany). Serum B-type natriuretic peptide (BNP) (ab108816, Abcam, Cambridge, UK) levels were quantified using an enzyme-linked immunosorbent assay kit. The concentration of empagliflozin in serum was measured using high-performance liquid chromatography (HPLC) as previously described [18].

2.3. Echocardiography

At the end of the study, the rats were examined by echocardiography (vevo 770TM-230, VisualSonics, Canada) in the parasternal long axis view by an experienced echocardiographer to collect data on the following parameters: interventricular septum in systole (IVSs), interventricular septum in diastole (IVSd), left ventricular end-systolic dimension (LVESd), left ventricular end-diastolic dimension (LVEDd), left ventricular posterior wall in systole (LVPWs), and left ventricular posterior wall in diastole (LVPWd). Further parameters were calculated using the following equations: Change in left ventricular posterior wall thickness (LVPW, %) = (LVPWs-LVPWd)/LVPWd*100 %; Change in interventricular septum thickness (IVS, %) = (IVSs-IVSd)/IVSd*100 %; Left ventricular end systolic volume (LVESV, mm^3) = 1.04*LVESd^3; Left ventricular end diastolic volume (LVEDV, mm^3)= 1.04*LVEDd^3; Stroke volume (SV, mm^3) = 1.04*LVEDd^3-1.04*LVESd^3; Fractional shortening (FS, %) = (LVEDd-LVESd)/LVEDd*100 %; Left ventricular ejection fraction (EF, %) = (1.04*LVEDd^3-1.04*LVESd^3)/(1.04*LVEDd^3) *100 %; Left ventricular mass (LVM) = 1.04* [(LVEDD+PWT+AWT) ^3 -LVEDD^3] [19,20].

2.4. Heart histological analysis

Heart tissue was embedded in paraffin after immersion for 48 h in 4 % paraformaldehyde and subsequently cut into 2 μm slices for Sirius Red staining, Periodic Schiff-Methyl Blue staining (PASM) and Masson's trichrome staining. Cardiomyocyte diameter was analyzed by measuring the diameter of 50 cardiomyocytes on each PASM-stained section and calculating the average. The percentage of myocardial fibrosis was obtained by analyzing Sirius Red stained slides using the ImageJ threshold method (National Institutes of Health), as described previously [21]. Analysis of perivascular fibrosis index was done by two blinded independent investigators using a semiquantitative grading score (grades I–IV) on Masson's trichrome stained slides as follows: I = weak, II= moderate, III = severe, and IV = very severe fibrosis. The media-to-lumen ratio of the vessels in the heart was assessed by measuring the vessel-wall area divided by the vessel-lumen area of all blood vessels in each PASM-stained section at 10 × magnification. The calculated mean value was used for further analysis. All analyses covered more than 80 % of the area of each slice.

2.5. Immunofluorescence staining

We performed immunofluorescence analysis using the following specific antibodies: CD68 (primary antibody: GB113109, Servicebio, China, dilution 1:2000; secondary antibody: GB22303, Servicebio, China, dilution 1:500), CD206 (primary antibody: GB113497, Servicebio, China, dilution 1:1000; secondary antibody: GB21303, Servicebio, China, dilution 1:300), INOS (primary antibody: GB11119, Servicebio, China, dilution 1:300; secondary antibody: GB21303, Servicebio, China, dilution 1:300), CD8 (primary antibody: GB11068, Servicebio, China, dilution 1:500; secondary antibody: GB21303, Servicebio, China, dilution 1:300), and CD4 (primary antibody: GB11064–1, Servicebio, China, dilution 1:500; secondary antibody: GB21303, Servicebio, China, dilution 1:300). Frozen Section (4 μm) were placed in the primary antibody at 4°C overnight. Then, the tissues and cells were washed and incubated with a secondary antibody. After staining the nuclei with 4′,6-Diamidino-2-phenylindole (DAPI), the tissues and cells were visualised. For each section, twelve randomized high-power fields were examined using a fluorescence microscope at 20x magnification. Cytotoxic T cells (CD8 +cells/Area) and helper T cells (CD4 +cells/Area), as well as the colocalisation of CD68/INOS and CD68/CD206 positive area were analysed using Aipathwell (Servicebio, China).

2.6. Single-nuclei RNA sequencing (snRNA-seq)

The collected heart tissues were quick-frozen in liquid nitrogen for 30 min and stored in a freezer at −80 °C. Based on the median of the final serum creatinine concentration, four heart samples from each group were selected for single-nuclei RNA sequencing (snRNA-seq). Nuclei were isolated by a custom protocol. In brief, frozen tissue specimens were chopped into small pieces and transferred into a pre-cooled gentleMACS C Tube (Miltenyi Biotec, Germany) prefilled with 4 ml of ice-cold lysis buffer [Nuclei Extraction Buffer (Miltenyi Biotec, Germany)]; 0.2 U/μl RNase Inhibitor (Sigma-Aldrich, USA)) without allowing the tissue to thaw. C Tubes were immediately transferred onto the gentleMACS™ Octo Dissociator (Miltenyi Biotec, Germany) for tissue homogenization and cell lysis by running program "4C_nuclei_1". The nuclei suspension was filtered through a 70 μm strainer and centrifuged at 300 g for 5 min at 4 °C. Supernatant was discarded and the nuclei pellet resuspended in 1.5 ml ice-cold lysis buffer. An aliquot of the nuclei suspension corresponding to 50–100 mg of the tissue input material was mixed with ice-cold lysis buffer for a total of 500 μL and transferred onto a Nuclei Isolation Column provided in the Chromium Nuclei Isolation Kit (10X Genomics, USA). All following steps were performed according to the manufacturer's instructions under the guidance of the Nuclei Isolation Protocol for Single-Cell Multiome ATAC + Gene Expression (CG000505). snRNA-seq libraries were prepared using the Chromium Next GEM Single Cell 3′ Kit v3.1 (10X Genomics, USA) according to the manufacturer's instructions. Briefly, high-quality sequencing data were obtained after a series of experimental procedures, including nuclei counting and quality control, gel beads-in-emulsion (GEMs) generation and barcoding, post-GEM-RT cleanup, cDNA amplification, gene expression library construction, and paired-end sequencing (read 1: 28 bp, read 2: 90 bp) on a NovaSeq 6000 platform (Illumina, USA). CellRanger (v7.0.0; 10X Genomics, USA) was applied to process the sequencing data and generate UMI-based gene count matrices. Reads were aligned to reference genome Rnor6.0 (Ensembl release 86). The Seurat R package (v4.1.3) was used for further downstream analyses. Cells were kept for downstream analysis if at least 350 genes were detected to exclude low-quality cells. Similarly, only genes detected in > 3 cells were kept for further analysis. Approximately

5000 nuclei per sample and 1100 genes per nuclei were detected. Transcript counts were normalized to 10,000 counts per cell and log-normalized using Seurat's "NormalizeData" function. Highly variable genes were identified by the "FindVariableFeatures" function applying the "vst" method and data were scaled using the "ScaleData" function. Cell clusters were determined via Seurat's default graph-based clustering strategy using the "FindNeighbors" and "FindClusters" functions. The top 40 principal components (PCs) and 1.45 resolution were used to compute the cell clusters. Forty-two cell clusters were identified in the dataset and represented via UMAP that was also calculated on the top 40 PCs. Cluster-based cell type annotation was performed on the expression of known marker genes which also identified clusters of cell multiplets and a single cluster representing low-quality nuclei that were removed for further analysis (Supplementary figure 1). To explore the heterogeneity in immune cell (IC), we performed secondary cluster analysis on lymphocytes and myeloid cells. Differential expression analysis was computed via the "FindAllMarkers" or "FindMarkers" function of the Seurat R package utilizing the MAST R package (Supplementary figure 2). Genes with an absolute fold change > 1.2 and an adjusted p value < 0.05 (Bonferroni correction) were considered differentially expressed genes (DEGs). Only genes detected in ≥ 10 % of the cells in at least one of the compared populations were considered for differential expression analysis. Pathway analysis [kyoto encyclopedia of genes and genomes (KEGG) and gene ontology (GO) analyses] was performed on the DEGs observed for ventricular cells using ClusterProfiler (3.10.1) R package. Enrichment of pathway and biological process was defined based on adjusted p value < 0.05. Three highly differentially expressed genes involved in regulating cardiomyocyte development were verified by quantitative real-time polymerase chain reaction (qRT-PCR). The DEGs data from the snRNA-seq analysis were obtained specifically from ventricular cardiomyocytes, whereas the qRT-PCR was performed on whole myocardial tissue, which includes ventricular cardiomyocytes as well as other types of cardiac cells.

2.7. Statistical information

GraphPad Prism version 10.0 and SPSS 26.0 software were used for statistical analysis and data visualisation. Outliers were identified and excluded using the ROUT method (Q = 1 %) in GraphPad Prism 10.0. For the statistical analysis of laboratory indicators, normally distributed data were analyzed using one-way ANOVA with Bonferroni's post hoc test, and non-normally distributed data were analyzed using Kruskal-Wallis test with Dunn's post hoc test. Differential gene-expression analysis was performed using Wilcoxon rank sum test. The false discovery rate (FDR) was controlled to correct for multiple testing. In all cases, differences were regarded as statistically significant if $p < 0.05$.

3. Results

3.1. Biochemical parameters indicated that Empagliflozin did not improve mild cardiac injury caused by 5/6 nephrectomy

After 95 days of 5/6 nephrectomy, serum creatinine and serum troponin T levels were significantly elevated, while serum BNP levels remained unchanged compared to controls (Table 1 and Fig. 1). There was no difference in blood pressure (BP) or heart rate between 5/6 nephrectomized rats and controls. Body weight, heart weight, and relative heart weight were also similar between the two groups. The telmisartan-treated group exhibited significantly lower heart weight than the 5/6 nephrectomy group, although serum troponin T and BNP levels did not differ between these groups (Table 1). Empagliflozin significantly reduced serum creatinine in 5/6 nephrectomy rats, but had no significant effect on BP, heart weight, serum troponin T or serum BNP. Heart rate was lower in the high-dose empagliflozin group compared to the 5/6Nx+PBO group (Table 1). 24 h after the last dose, the plasma empagliflozin concentration in the high-dose group was 23.20 ± 6.50 ng/ml, a concentration that was well above its half maximal inhibitory concentration (3.1 ng/ml) [17]. The mortality rate for each group was as follow: Sham + Placebo (12.50 %), 5/6Nx + Placebo (40.00 %), 5/6Nx + 3 mg Empagliflozin (30.77 %), 5/6Nx + 15 mg Empagliflozin (21.43 %), and 5/6Nx + Telmisartan (30.0 %). Mortality analyses revealed no significant differences between groups, so these data are not presented graphically (Supplementary file 1).

3.2. Echocardiography showed that Empagliflozin reduced LVPWs and IVSd, but had no effect on SV, EF and FS

After 95 days of 5/6 nephrectomy, stroke volume (SV), left ventricular ejection fraction (EF) and fractional shortening (FS) and left ventricular mass (LVM) were increased in rats (Table 2; Fig. 1). Left ventricular posterior wall in systole (LVPWs), left ventricular posterior wall in diastole (LVPWd), change in left ventricular posterior wall thickness (LVPW), interventricular septum in systole (IVSs), interventricular septum in diastole (IVSd) and change in interventricular septum thickness (IVS) parameters were not different from those of normal rats (Table 2). Telmisartan treatment reduced LVPWs, SV and LVM. Empagliflozin treatment also decreased LVPWs, IVSd and LVM (Fig. 1D), but had no effect on cardiac pumping function. SV, EF and FS in the empagliflozin group were not different from those in the 5/6Nx+PBO group (Table 2; Fig. 1E-G).

Table 1
Animal characteristics.

Parameters	Sham + PBO (n = 7)	5/6Nx + PBO (n = 9)	5/6Nx + 3 mg EMPA (n = 9)	5/6Nx + 15 mg EMPA (n = 11)	5/6Nx + TELM (n = 7)
Final body weight (g)	509.00 ± 18.09	464.11 ± 17.58	494.56 ± 16.37	468.18 ± 13.11	475.29 ± 11.36
Heart weight (g)	1.87 ± 0.10	1.82 ± 0.10	1.64 ± 0.05	1.73 ± 0.10	1.37 ± 0.06**
Rel. heart weight [10–2]	0.37 ± 0.01	0.39 ± 0.03	0.33 ± 0.01	0.37 ± 0.02	0.29 ± 0.01**
Final SBP (mmHg)	164.17 ± 7.06	163.00 ± 7.84	166.00 ± 8.62	164.33 ± 23.92	130.67 ± 28.43
Final DBP (mmHg)	86.67 ± 14.61	76.38 ± 13.89	95.33 ± 28.72	40.00 ± 4.04	70.33 ± 4.63
Final heart rate (bpm)	397.50 ± 28.16	382.88 ± 28.83	387.33 ± 47.19	248.33 ± 7.69*	372.67 ± 26.85
Final serum creatinine (μmol/L)	24.00 ± 1.51****	72.00 ± 8.49	47.50 ± 4.98**	49.09 ± 2.76**	54.86 ± 2.42
Final serum troponin T (ng/L)	0.01 ± 0.003**	0.04 ± 0.009	0.02 ± 0.005	0.03 ± 0.004	0.03 ± 0.004
Final serum BNP (ng/ml)	0.20 ± 0.03	0.25 ± 0.05	0.24 ± 0.01	0.23 ± 0.03	0.21 ± 0.03
T24 (Empagliflozin, ng/ml)	-	-	< 2.00	23.20 ± 6.50	-

Note: Rel. heart weight (Relative heart weight) = Heart weight / final body weight; SBP: Systolic blood pressure; DBP: Diastolic blood pressure; BNP: Serum B-type natriuretic peptide; T24 (Empagliflozin, ng/ml): Plasma concentrations of empagliflozin 24 h after the last dose. -: Below the minimum detection value (2 ng/ml). Sham: Sham operation; 5/6Nx: 5/6 nephrectomized rat model; PBO: Placebo; TELM: Telmisartan; EMPA: Empagliflozin. Values displayed are mean ± SEM. *$p < 0.05$; **$p < 0.01$; ****$p < 0.0001$, significantly different from 5/6Nx + PBO. Normally distributed data were analyzed using one-way ANOVA with Bonferroni's post hoc test, and non-normally distributed data were analyzed using Kruskal-Wallis test with Dunn's post hoc test.

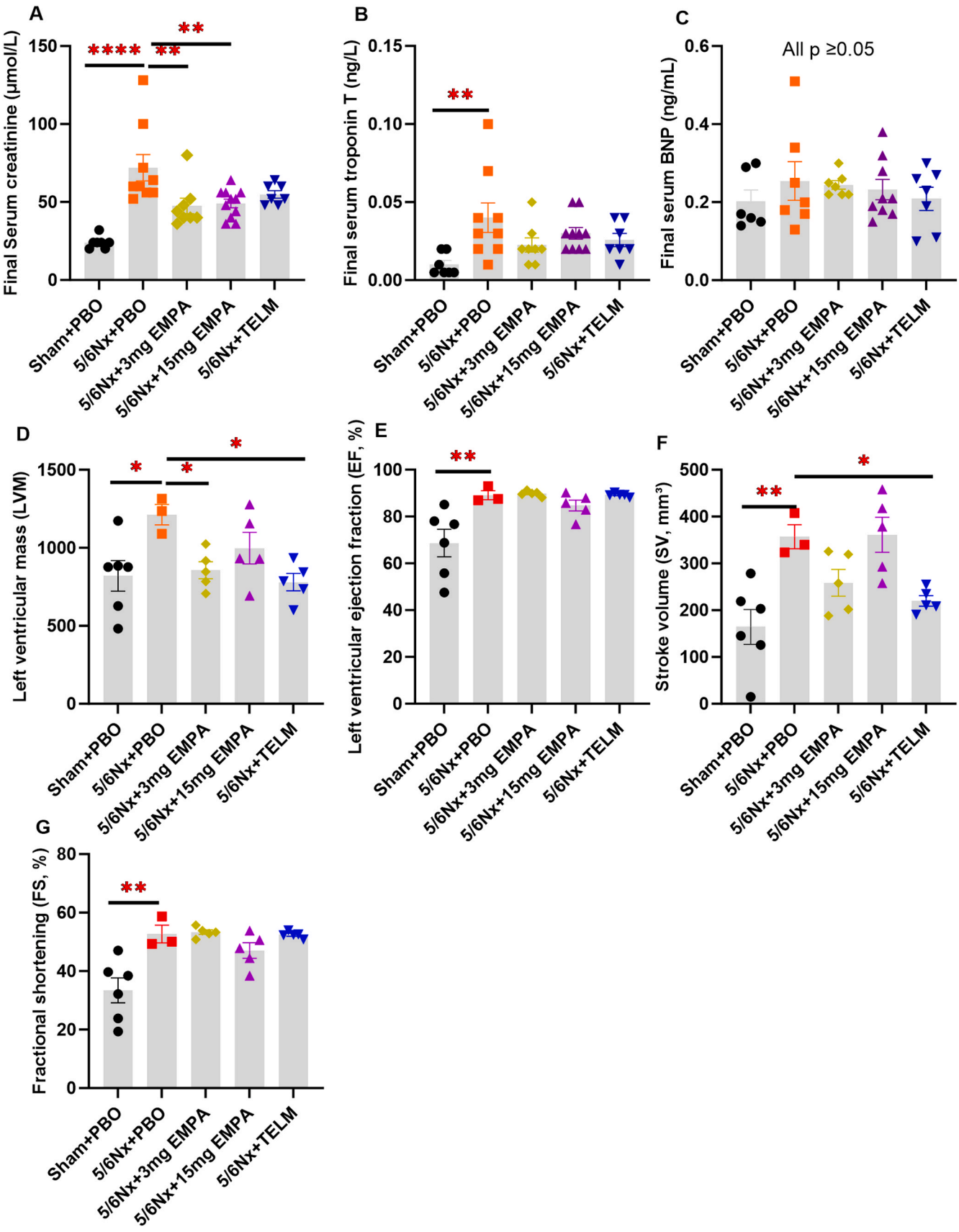

(caption on next page)

Fig. 1. Effects on cardiac and renal function compared to 5/6Nx + PBO group. (A) Final serum creatinine (μmol/L): Sham + PBO (n = 7); 5/6Nx + PBO(n = 9); 5/6Nx + 3 mg EMPA (n = 8); 5/6Nx + 15 mg EMPA (n = 11); 5/6Nx + TELM (n = 7). (B) Final serum troponin T (ng/L): Sham + PBO (n = 7); 5/6Nx + PBO(n = 9); 5/6Nx + 3 mg EMPA (n = 8); 5/6Nx + 15 mg EMPA (n = 10); 5/6Nx + TELM (n = 7). (C) Final serum BNP (ng/ml): Sham + PBO (n = 6); 5/6Nx + PBO(n = 7); 5/6Nx + 3 mg EMPA (n = 7); 5/6Nx + 15 mg EMPA (n = 9); 5/6Nx + TELM (n = 7). (D) Left ventricular mass (LVM). (E) Left ventricular ejection fraction (EF). (F) Stroke volume (SV). (G) Fractional shortening (FS). (D-G) Sham + PBO (n = 6); 5/6Nx + PBO(n = 3); 5/6Nx + 3 mg EMPA (n = 5); 5/6Nx + 15 mg EMPA (n = 5); 5/6Nx + TELM (n = 5). Sham: Sham operation; 5/6Nx: 5/6 nephrectomized rat model; PBO: Placebo; TELM: Telmisartan; EMPA: Empagliflozin. Values displayed are mean ± SEM. *p < 0.05; **p < 0.01; ****p < 0.0001, significantly different from 5/6Nx + PBO. Normally distributed data were analyzed using one-way ANOVA with Bonferroni's post hoc test, and non-normally distributed data were analyzed using Kruskal-Wallis test with Dunn's post hoc test.

Table 2
Cardiac echocardiographic data.

Parameters	Sham + PBO (n = 6)	5/6Nx + PBO (n = 3)	5/6Nx+ 3mgEMPA (n = 5)	5/6Nx+ 15mgEMPA (n = 5)	5/6Nx + TELM (n = 5)
Left ventricular posterior wall in systole (LVPWs, mm)	2.83 ± 0.19	3.33 ± 0.09	2.64 ± 0.10*	2.90 ± 0.13	2.48 ± 0.11**
Left ventricular posterior wall in diastole (LVPWd, mm)	2.05 ± 0.10	2.00 ± 0.15	1.80 ± 0.08	1.78 ± 0.14	1.76 ± 0.11
Change in left ventricular posterior wall thickness (LVPW, %)	38.92 ± 9.05	68.89 ± 14.88	47.52 ± 7.17	65.28 ± 9.31	43.19 ± 10.52
Interventricular septum in systole (IVSs, mm)	3.00 ± 0.25	2.67 ± 0.09	2.62 ± 0.12	2.40 ± 0.09	2.50 ± 0.09
Interventricular septum in diastole (IVSd, mm)	2.08 ± 0.11	2.30 ± 0.12	2.02 ± 0.06	1.88 ± 0.09*	2.00 ± 0.08
Change in interventricular septum thickness (IVS, %)	43.47 ± 6.10	16.68 ± 8.33	30.78 ± 9.69	28.21 ± 4.78	25.30 ± 3.15
Left ventricular end systolic volume (LVESV, mm3)	60.08 ± 13.08	42.68 ± 5.85	28.93 ± 2.51	68.69 ± 15.84	26.52 ± 1.39
Left ventricular end diastolic volume (LVEDV, mm3)	224.39 ± 43.19*	399.72 ± 20.05	287.46 ± 30.82	429.66 ± 49.88	246.27 ± 12.28
Stroke volume (SV, mm^3)	164.31 ± 37.32**	357.04 ± 25.78	258.53 ± 28.61	360.97 ± 37.57	219.75 ± 11.18*
Left ventricular ejection fraction (EF, %)	68.67 ± 5.88**	89.13 ± 1.91	89.79 ± 0.52	84.70 ± 2.34	89.21 ± 0.34
Fractional shortening (FS, %)	33.42 ± 4.25**	52.65 ± 3.01	53.32 ± 0.79	47.05 ± 2.65	52.42 ± 0.50
Left ventricular mass (LVM)	819.93 ± 97.82*	1212.62 ± 65.90	856.01 ± 54.63*	997.65 ± 101.30	779.87 ± 55.65*

Note: Change in left ventricular posterior wall thickness (LVPW, %) = (LVPWs-LVPWd)/LVPWd*100 %; Change in interventricular septum thickness (IVS, %) = (IVSs-IVSd)/IVSd*100 %; Left ventricular end systolic volume (LVESV, mm^3) = 1.04*LVESd$^{\hat{}}$3; Left ventricular end diastolic volume (LVEDV, mm^3)= 1.04*LVEDd$^{\hat{}}$3; Stroke volume (SV, mm^3) = 1.04*LVEDd$^{\hat{}}$3-1.04*LVESd$^{\hat{}}$3; Fractional shortening (FS, %) = (LVEDd-LVESd)/LVEDd*100 %; Left ventricular ejection fraction (EF, %) = (1.04*LVEDd$^{\hat{}}$3-1.04*LVESd$^{\hat{}}$3)/(1.04*LVEDd$^{\hat{}}$3)*100 %; Left ventricular mass (LVM) = 1.04* [(LVEDD+PWT+AWT) $^{\hat{}}$3 -LVEDD$^{\hat{}}$3]. Sham: Sham operation; 5/6Nx: 5/6 nephrectomized rat model; PBO: Placebo; TELM: Telmisartan; EMPA: Empagliflozin. Values displayed are mean ± SEM. *p < 0.05; **p < 0.01, significantly different from 5/6Nx + PBO. Normally distributed data were analyzed using one-way ANOVA with Bonferroni's post hoc test, and non-normally distributed data were analyzed using Kruskal-Wallis test with Dunn's post hoc test.

3.3. Histological parameters revealed that empagliflozin significantly improved the enlargement of cardiomyocytes caused by 5/6 nephrectomy but had no effect on myocardial fibrosis

Fig. 2 shows heart tissue stained with PASM and Masson. Histological analysis showed that 5/6 nephrectomy resulted in enlarged cardiomyocytes, thickened vascular walls, and increased perivascular fibrosis, but did not increase myocardial fibrosis (Fig. 2). Treatment with telmisartan and both doses of empagliflozin significantly improved cardiomyocyte enlargement caused by 5/6 nephrectomy, but had no effect on vascular wall thickness, perivascular fibrosis, or myocardial fibrosis (Fig. 2).

3.4. snRNA-seq analysis indicated that empagliflozin did not change the cell composition of heart in 5/6 nephrectomy rats

Four heart samples from each group were selected around the median serum creatinine level to generate a snRNA-seq atlas (Fig. 3A). A total of 82,352 nuclei were detected, with the number of nuclei detected per sample ranging from 3793 to 6094. Cluster analysis identified 41 cell clusters. Approximately 1100 genes were identified in each nucleus. Based on gene expression markers (Supplementary file 2), 17 cell types were identified and are marked in Fig. 3B. The cell composition analysis of each group revealed that cardiomyocytes (ventricular), endocardial cells, and fibroblasts constituted the majority of cells in all groups (Fig. 3C). No significant differences in the proportions of ventricular cardiomyocytes, atrial cardiomyocytes, epicardial cells, endocardial cells, myeloid cells, lymphoid cells, proliferation_cells, proliferation _ immune cells, and fibroblasts were observed among the groups (Fig. 3 D-K). To further explore immune cell heterogeneity, we performed secondary cluster analysis on lymphocytes and myeloid cells (Supplementary figure 2; Supplementary file 3). The data revealed no significant differences in immune cell populations between normal rats and 5/6 nephrectomy rats, and therefore, we did not address this further in the article.

3.5. qRT-PCR confirmed empagliflozin-mediated regulation of cardiomyocyte development genes Fhl2, Tbx20, and Angpt1

DEGs for each cell type in each group can be found in Supplementary file 4. According to the criteria of absolute fold change > 1.2 and an adjusted p value < 0.05, 44 DEGs were identified in ventricular cardiomyocytes from the 5/6Nx + 15 mg empagliflozin group compared to 20 DEGs in the 5/6Nx + PBO group. Pathway analysis was conducted using the KEGG and GO databases as reference. The top 15 most significant biological processes (adjusted p value < 0.05) are shown in Fig. 4A. These indicate that four biological processes related to heart development were regulated, including heart development, circulatory system development, cardiac muscle cell differentiation, and cardiac muscle tissue development. Among these regulated biological processes, the three genes with the greatest difference in expression between the control and experimental groups and an involvement in cardiomyocyte development, *Fhl2* (Four and a half LIM domains 2), *Tbx20* (T-Box transcription factor 20), and *Angpt1* (Angiopoietin 1), were validated by qRT-PCR (Fig. 4 B, C, D). qRT-PCR confirmed that empagliflozin increased *Fhl2* and decreased *Tbx20* expression (Fig. 4 B, 4C). However, conflicting results were observed for *Angpt1* (Fig. 4 D), likely due to the difference in sample sources: the snRNA-seq data was obtained from

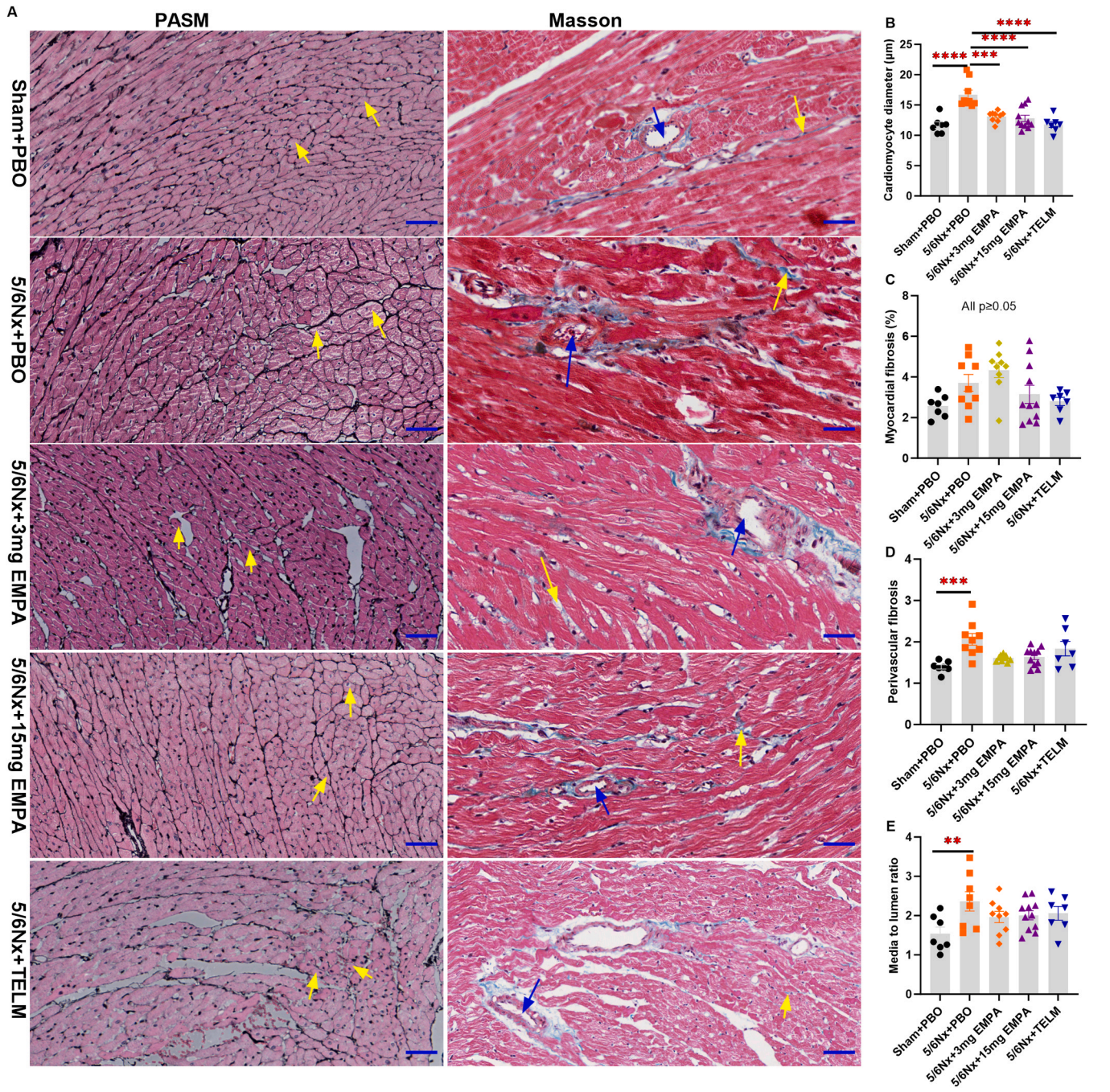

Fig. 2. Effect on cardiac histology. (A) Representative micrographs of PASM and Masson staining of heart sections from each group (X400, Scale bar=50μm); Yellow arrows in PASM: cardiomyocytes; Blue arrows in Masson: myocardial vessels; Yellow arrows in Masson: myocardial fibrosis. (B) Cardiomyocyte diameter (μm). (C) Myocardial fibrosis (%). (D) Perivascular fibrosis. (E) Media to lumen ratio. Sham + PBO (n = 7); 5/6Nx + PBO(n = 9); 5/6Nx + 3 mg EMPA (n = 9); 5/6Nx + 15 mg EMPA (n = 11); 5/6Nx + TELM (n = 7). Sham: Sham operation; 5/6Nx: 5/6 nephrectomized rat model; PBO: Placebo; TELM: Telmisartan; EMPA: Empagliflozin. Values displayed are mean ± SEM. **p < 0.01; ***p < 0.001; ****p < 0.0001, significantly different from 5/6Nx + PBO. Normally distributed data were analyzed using one-way ANOVA with Bonferroni's post hoc test, and non-normally distributed data were analyzed using Kruskal-Wallis test with Dunn's post hoc test.

ventricular cardiomyocytes, whereas the qRT-PCR was conducted on whole myocardial tissue. Furthermore, the relatively lower gene expression difference may also be one of the reasons for the discrepancy between the qRT-PCR and snRNA-seq analysis results of Angpt1 (5/6Nx + 15 mg EMPA: fold change = 1.77, adjusted p value < 0.0001; 5/6Nx + PBO: fold change = 0.74, adjusted p value < 0.0001).

3.6. Immunofluorescence analysis indicated that empagliflozin increased the infiltration of M2 macrophages, CD4+ T cells and CD8+ T cells in cardiac tissue in 5/6 nephrectomy rats

Empagliflozin's cardioprotective effect has been linked to modulation of the M1/M2 macrophage balance [22–25]. In our previous study [23], we also found that empagliflozin inhibited the polarization of CD206-CD68- M2 macrophages to CD206+CD68+ M2 macrophages. Thus, we examined cardiac M1 macrophages (CD68+ INOS+) and M2

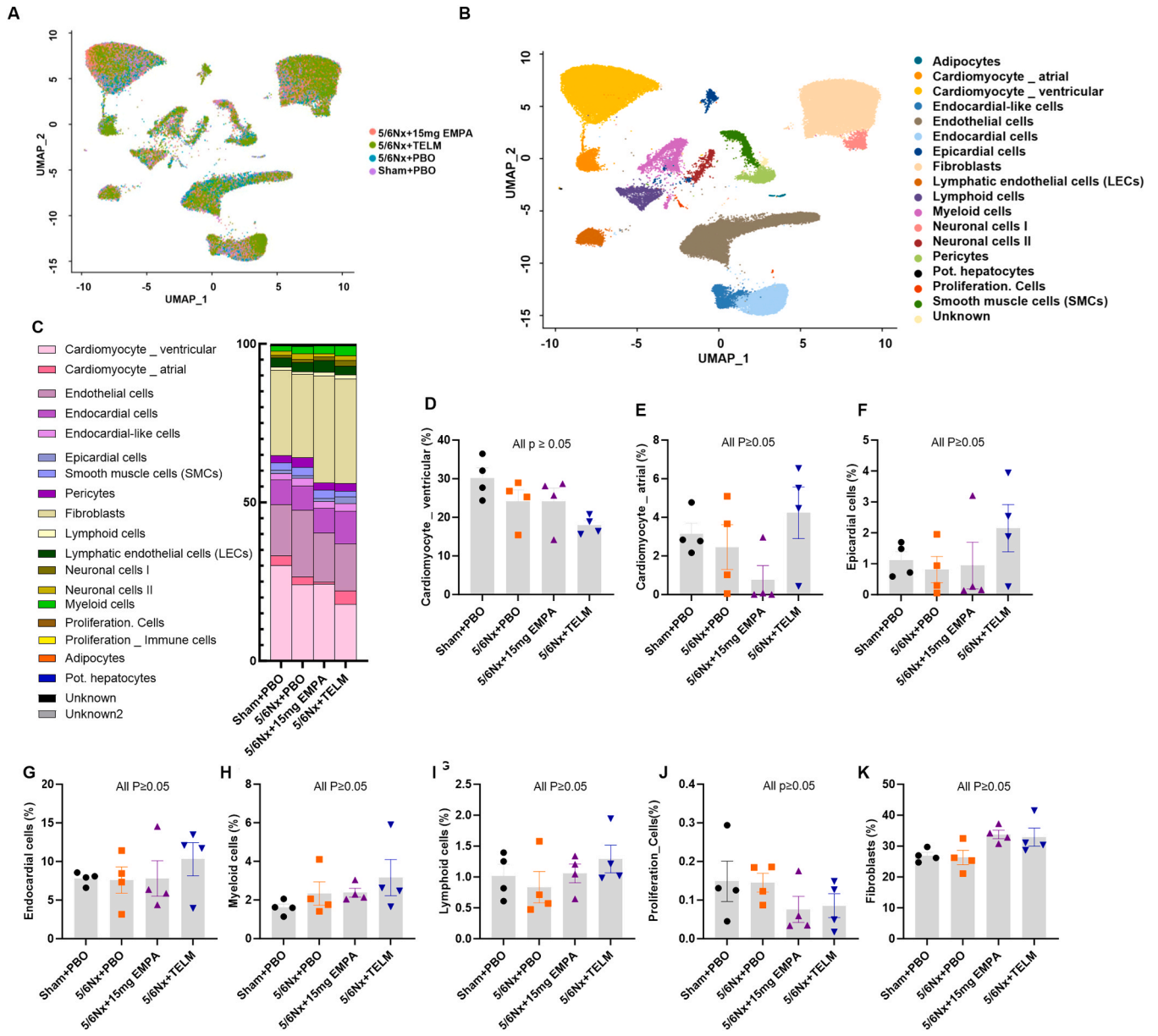

Fig. 3. snRNA-seq identified the major cell types in heart. (A) UMAP embeddings of snRNA-seq data colored by group batches. (B) Dimensionality reduction and clustering of 82352 cells. 41 cell clusters were identified. (C) Stacked bar graphs depicting the alterations in the percentage of different cell clusters between groups. (D-K) Comparison of the percentage of different cell clusters in each group. Sham: Sham operation; 5/6Nx: 5/6 nephrectomized rat model; PBO: Placebo; TELM: Telmisartan; EMPA: Empagliflozin. Values displayed are mean ± SEM. All groups were compared with the 5/6NX+PBO group, and a p-value of < 0.05 was considered statistically significant. One-way ANOVA with Bonferroni's post hoc test was used for between-group comparisons.

macrophages (CD68+ CD206+) by immunofluorescence. M1 and M2 macrophage levels in 5/6Nx rats were similar to controls, but M2 macrophage levels were significantly increased in empagliflozin-treated rat (Fig. 5C). Furthermore, CD4+ T cells and CD8+ T cells play an important role in CKD [26,27], so we also analysed the number of CD4+ T cells and CD8+ T cells in heart using immunofluorescence (Fig. 5 A). CD4+ T cell numbers were unchanged between 5/6Nx and control rats, but significantly increased in the high-dose empagliflozin group (Fig. 5 D). Low-dose empagliflozin restored CD8+ T cell numbers, although variability among groups was high. (Fig. 5 E). Overall, only very small numbers of CD4+ T cells and CD8+ T cells were detected in each group (Fig. 5 ADE).

4. Discussion

This study provides compelling evidence for the cardioprotective effects of Empagliflozin in a non-diabetic cardiorenal syndrome model induced by 5/6 nephrectomy. By integrating high-level functional analysis (echocardiography), single-cell RNA sequencing, and detailed morphological assessments, we demonstrate that Empagliflozin significantly attenuates LVM and cardiomyocyte hypertrophy. Echocardiography revealed reductions in LVPWs and IVSd, consistent with structural improvements. Histological analysis confirmed these findings, showing reduced cardiomyocyte diameter, while single-cell RNA sequencing identified critical molecular pathways involving *Fhl2*, *Tbx20*, and *Angpt1*, which regulate cardiomyocyte development and myocardial remodeling. Importantly, these changes occurred without affecting echocardiographic heart function, as evidenced by unchanged SV, EF,

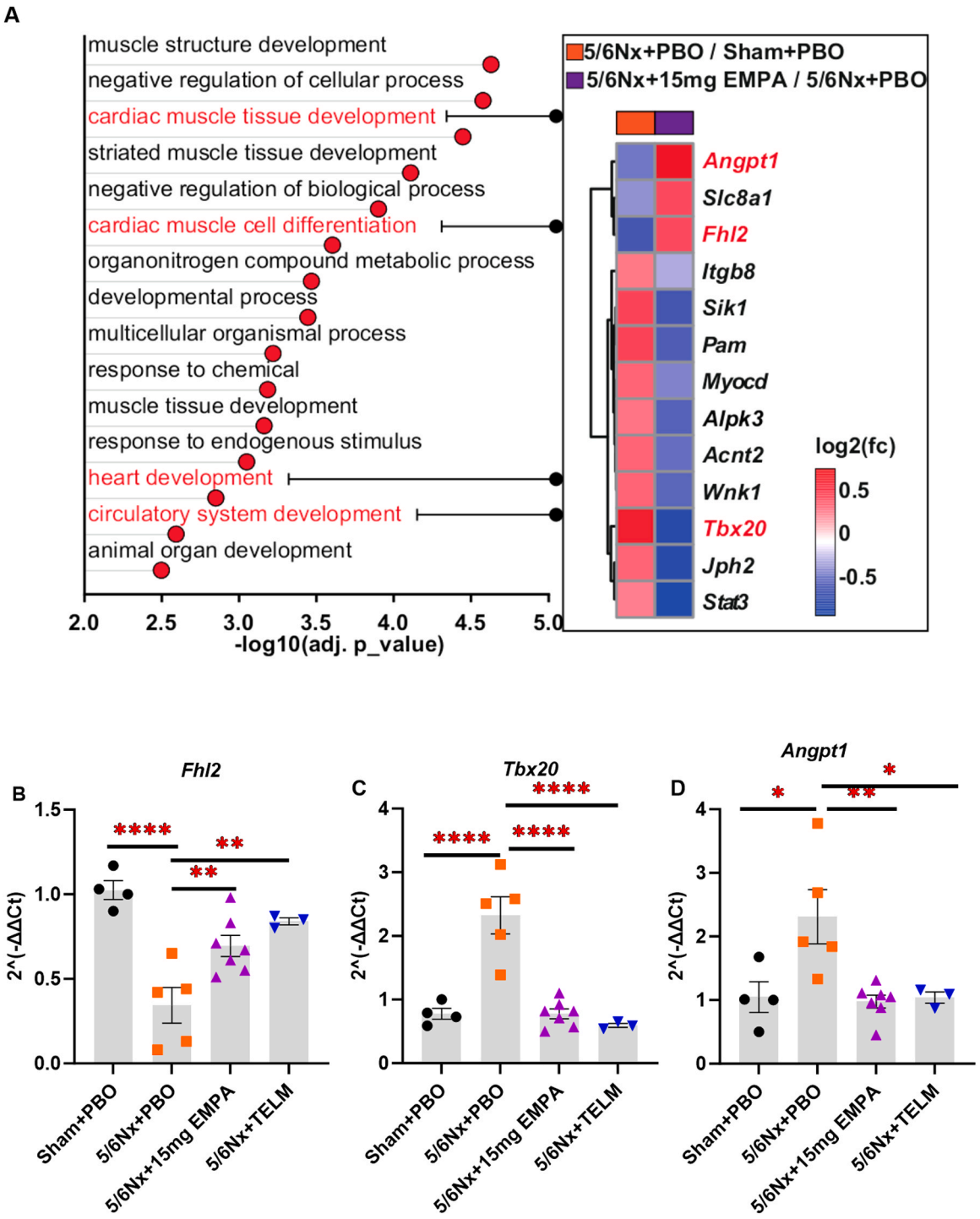

Fig. 4. Differentially expressed genes (DEGs) in cardiomyocyte _ ventricular and quantitative real-time polymerase chain reaction (qRT-PCR). (A) Left panel: Gene ontology analyses of differentially expressed genes (DEGs) in single-nuclei RNA sequencing data. The top 15 biological processes with an adjusted $p < 0.05$ are displayed, sorted from lowest to highest adjusted p value. Right panel: Heatmap of DEGs for biological processes related to heart development. (B-D) qRT-PCR validation of Fhl2 (Four and a half LIM domains 2), Tbx20 (T-Box transcription factor 20), and Angpt1 (Angiopoietin 1). Sham: Sham operation; 5/6Nx: 5/6 nephrectomized rat model; PBO: Placebo; TELM: Telmisartan; EMPA: Empagliflozin. Values displayed are mean ± SEM. *$p < 0.05$; **$p < 0.01$; ****$p < 0.0001$, significantly different from 5/6Nx + PBO. One-way ANOVA with Bonferroni's post hoc test was used for between-group comparisons.

and FS. Together, these findings underscore Empagliflozin's potential to mitigate cardiac remodeling in cardiorenal syndrome, independent of hemodynamic changes or ion channel modulation. By combining functional, molecular, and morphological approaches, this study offers a comprehensive understanding of Empagliflozin's cardioprotective mechanisms and extends its therapeutic potential beyond diabetes management to broader clinical contexts, including cardiorenal syndrome.

Left ventricular hypertrophy (LVH) is the most common early cardiac structural abnormality observed in patients with chronic kidney disease (CKD) [2]. Several clinical trials have demonstrated that SGLT2 inhibitors can reduce LVM [11,14,28]. Notably, the EMPA-HEART Cardiolink-6 trial found that empagliflozin effectively reduces myocardial hypertrophy even in patients without pre-existing hypertrophy [14].

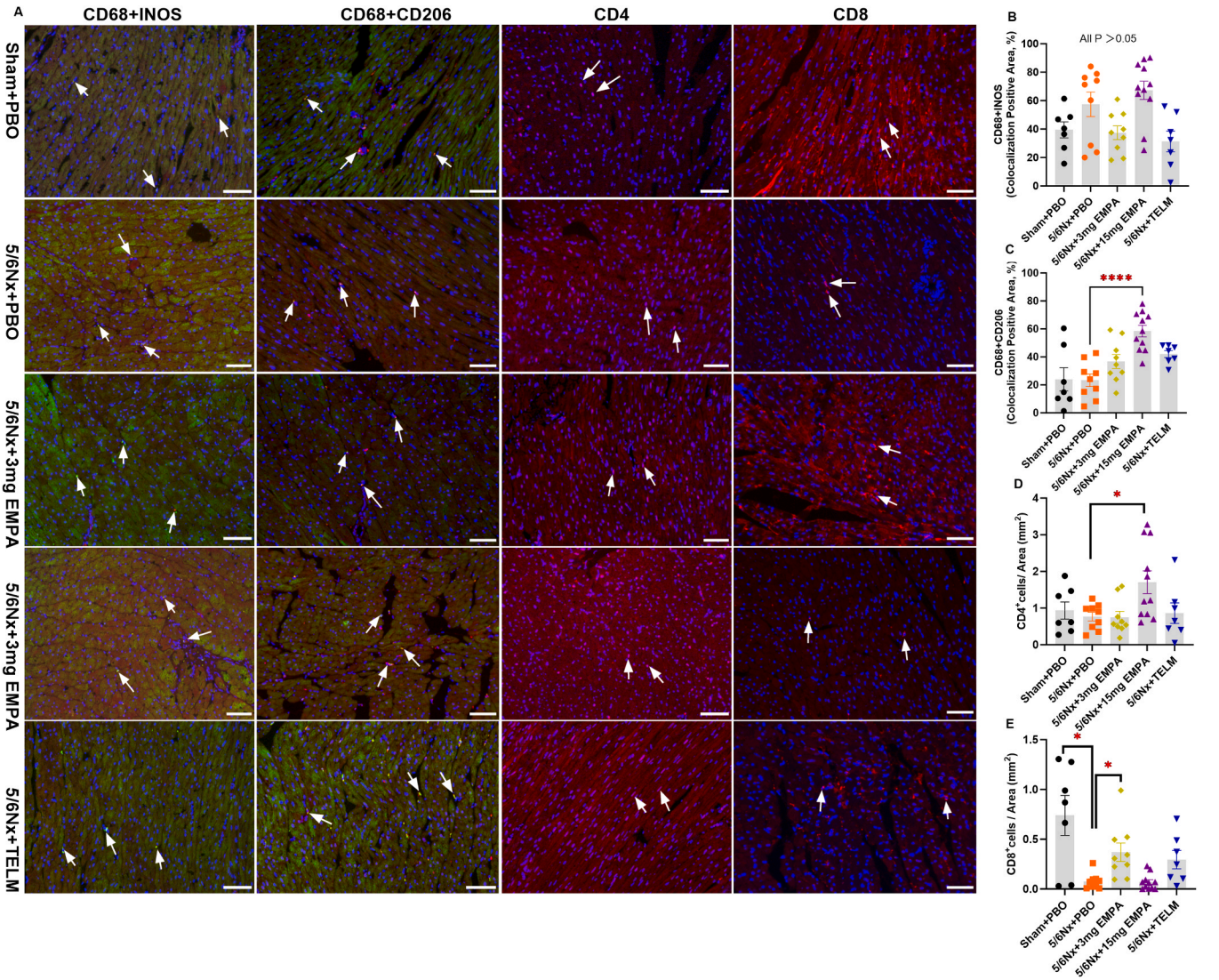

Fig. 5. Effects of Empagliflozin on macrophage, CD4 + T cell and CD8 + T cell in heart. (A) Representative micrographs of heart sections from each group (X200, Scale bar=100μm); (B) M1 Macrophages (CD68 + INOS+). (C) M2 Macrophages (CD68 + CD206 +). (D) CD4 + T cell. (E) CD8 + T cell. Sham + PBO (n = 7); 5/6Nx + PBO(n = 9); 5/6Nx + 3 mg EMPA (n = 9); 5/6Nx + 15 mg EMPA (n = 11); 5/6Nx + TELM (n = 7). Sham: Sham operation; 5/6Nx: 5/6 nephrectomized rat model; PBO: Placebo; TELM: Telmisartan; EMPA: Empagliflozin. Values displayed are means ± SEM. *$p < 0.05$; ****$p < 0.0001$, significantly different from 5/6Nx + PBO. One-way ANOVA with Bonferroni's post hoc test was used for between-group comparisons. Normally distributed data were analyzed using one-way ANOVA with Bonferroni's post hoc test, and non-normally distributed data were analyzed using Kruskal-Wallis test with Dunn's post hoc test.

Similarly, the DAPA-LVH trial revealed that patients with higher baseline LVM experienced a more significant reduction in LVM following empagliflozin treatment [13]. Additionally, numerous preclinical studies have highlighted the beneficial effects of SGLT2 inhibitors on myocardial hypertrophy [29–31]. However, the precise mechanisms through which SGLT2 inhibitors modulate myocardial remodeling remain unclear. In our study, we investigated the effects of empagliflozin on myocardial hypertrophy and its potential mechanisms in a non-diabetic heart-kidney syndrome model for the first time. Our findings also revealed that after 5/6 nephrectomy, both cardiac function (evidenced by elevated serum troponin T) and morphology (manifested as increased cardiomyocyte diameter) were disrupted. Some early hypotheses suggested that reducing the preload and afterload on the heart was the key mechanism through which ARBs and SGLT2 inhibitors improve cardiac structure and function. However, in this study, we observed that Empagliflozin had effects independent of blood pressure changes. Recent studies have also pointed out that the reduction in LVM is unrelated to changes in blood pressure. The EMPA-HEART CardioLink-6 Randomized Clinical Trial showed that changes in 24-hour ambulatory blood pressure were not associated with changes in LVM over a 6-month observation period [14]. In the Hypertension (LIFE) Trial, the Losartan treatment group (compared to Atenolol) showed a greater reduction in LVM and cardiovascular events, but there were no significant differences in blood pressure between the two treatment groups (Losartan and Atenolol) [32]. Furthermore, some studies have suggested that left ventricular mass is not always correlated with higher blood pressure levels [33]. Research by Paneni, F. et al. also suggested that SGLT2 inhibitors can reduce left ventricular hypertrophy independently of preload reduction [34]. These observations suggest that, in addition to affecting hemodynamics, the reduction in LVM observed after Empagliflozin treatment may involve alternative mechanisms.

We used snRNA sequencing technology to examine the gene expression in ventricular cardiomyocytes. Empagliflozin regulated some genes that were abnormally expressed in ventricular cardiomyocytes due to 5/6 nephrectomy. These genes are mainly involved in the regulation of cardiomyocyte development. regulating the development of cardiomyocytes. We performed qRT-PCR validation on the two genes with the most significant expression differences (*Fhl2* and *Tbx20*). The

results showed that Empagliflozin upregulated the expression of *Fhl2* while downregulating the expression of *Tbx20*. *Fhl2* is mainly expressed in the heart and plays a protective role in pathological cardiac hypertrophy [35]. In human hypertrophic cardiomyopathy (HCM) samples and HCM mouse models, Fhl2 levels are significantly reduced [36]. Compared to wild-type mice, Fhl2 knockout amplified the mice's hypertrophic response to Ang II/isoproterenol, including significant increases in cardiomyocyte cross-sectional area, heart weight ratio, and LVM [37,38]. Overexpression of Fhl2, on the other hand, reduced adrenergic-induced cardiac hypertrophy [39]. Fhl2 may be an important negative regulator of key signaling pathways in myocardial hypertrophy, such as mitogen-activated protein kinase (MAPK)/extracellular signal-regulated kinase (ERK) and calcineurin/nuclear factor of activated T cells (NFAT). Fhl2 interacts with ERK2 and calcineurin on the sarcomere to inhibit MAPK/ERK and calcineurin/NFAT signaling [38]. MAPK/ERK regulates various biological functions, including cardiomyocyte differentiation and growth, but the downstream mechanisms remain inadequately understood. In our study, we did not validate the downstream factors of Fhl2, but we confirmed the expression of Fhl2 in ventricular cardiomyocytes through both snRNA sequencing and qRT-PCR. It is likely that Empagliflozin restores the inhibition of myocardial hypertrophy signaling pathways, which are disrupted by 5/6 nephrectomy, through upregulation of Fhl2.

Next, we explored whether Empagliflozin affects cardiomyocyte number. Traditional views hold that adult cardiomyocytes have completed differentiation and have limited proliferative ability. However, recent studies suggest that genes involved in regulating heart development during the embryonic stage are reactivated in adult heart pathological conditions and promote cardiac regeneration [40]. The T-box transcription factor 20 (Tbx20) gene is a key regulator of cardiomyocyte proliferation during embryonic development [41]. Tbx20 protein is highly expressed in the free wall of the adult left ventricle and the interventricular septum [42]. Current views suggest that Tbx20 is also necessary for adult heart homeostasis [43]. One study analyzed the genome-wide DNA and transcriptomic data from Tbx20 knockout mice. The results showed that knocking out the Tbx20 gene in the adult mouse heart led to the upregulation/downregulation of over 4000 genes, highlighting the importance of Tbx20 in the adult heart. This study also pointed out that Tbx20 regulates active anti-proliferation programs in the adult heart [44]. Inducing Tbx20 overexpression in the adult mouse heart was shown to suppress negative cell-cycle regulators (p21, Meis1, Btg2) and promote cardiomyocyte proliferation without altering heart morphology or pathology, including no induction of cardiac hypertrophy, fibrosis, or dysfunction [45]. They believed this was because Tbx20-induced proliferation mainly resulted in small-volume mononucleated cardiomyocytes, so overexpression of Tbx20 in the adult heart did not affect the normal size of the heart [45]. Most studies currently suggest that Tbx20 mediates adult cardiomyocyte proliferation by activating the Bone Morphogenetic Protein 2 (BMP2)/phosphorylated Smad (pSmad)1/5/8 signaling pathway [46], but it remains unclear whether Tbx20-induced cardiomyocyte proliferation further leads to cardiac hypertrophy. In various experimental models, including hyperglycemia-induced cardiomyocyte proliferation [46], chronic hypoxia-induced right ventricular hypertrophy [47], an increase in cardiac Tbx20 expression is observed, and improvements in cardiac function are accompanied by a decrease in Tbx20 expression [47]. In our study, after 3 months of 5/6 nephrectomy, rats showed an increase in LV mass and cardiomyocyte diameter accompanied by an increase in Tbx20 expression. However, snRNA sequencing data showed no increase in the number of cardiomyocytes (ventricular and atrial) or other non-cardiomyocytes (epicardial cells, endocardial cells, myeloid cells, lymphoid cells, and fibroblasts) in 5/6 nephrectomized rats compared to normal rats. This is inconsistent with the current view that Tbx20 promotes small-volume cardiomyocyte proliferation. Empagliflozin's effect on improving cardiomyocyte enlargement and LVM was also accompanied by a decrease in Tbx20 expression, which is similar to the observation by Vanderpool RR. et al., where improvements in cardiac function following treatment were accompanied by a decrease in Tbx20 expression [47]. Based on the current data, we speculate that Tbx20 is involved in the myocardial injury induced by 5/6 nephrectomy, but rather through other mechanisms than through influencing cardiomyocyte proliferation. The reduction in Tbx20 following Empagliflozin treatment may be a secondary effect, possibly mediated by the upregulation of Fhl2. A study by Sengupta, A. et al. reported thatTbx20 expression increases during the acute phase of adult myocardial ER stress but decreases during prolonged ER stress, suggesting that the role of Tbx20 in myocardial pathology is dynamic and context-dependent [46].

Some recent studies reported that the beneficial effects of SGLT2 inhibitors are related to their modulation of macrophage differentiation and polarization [48]. During myocardial injury, monocytes are recruited to the damaged area and differentiate into pro-inflammatory M1 macrophages (CD68+/INOS+), promoting local inflammatory responses. M1 macrophages then further differentiate into anti-inflammatory/pro-fibrotic M2 macrophages (CD68+/CD206+), promoting tissue repair and collagen deposition. Therefore, the ratio of M1 and M2 macrophages at different stages of disease may influence disease outcomes. Some studies have reported that SGLT2 inhibitors can reduce macrophage, CD4+ T cell, and B cell infiltration in ischemic myocardium and atherosclerotic plaque areas [24,49]. Some studies support that SGLT2 inhibitors promote macrophage polarization towards the M2 phenotype and suppress inflammation [24]. In another study of ours using single-cell sequencing technology, we found that empagliflozin inhibited the polarization of M1 to M2 macrophages [23]. In this study, snRNA sequencing results showed that empagliflozin, in addition to reducing monocytes/neutrophils, had no effect on macrophages and T cells. Due to the limited sample size of the snRNA sequencing, we performed further validation using immunofluorescence staining. These analyses revealed that empagliflozin increased the infiltration of M2 macrophages, CD4+ T cells, and CD8+ T cells in the myocardium of 5/6 nephrectomized rats. However, the number of these immune cells in 5/6 nephrectomized rats was not significantly different from that in normal rats. In addition, a high degree of variability was observed in $CD8^+$ T cell numbers in the sham+PBO group. Furthermore, since our study lasted more than 3 months, it is possible that macrophages and T cells no longer play a dominant role in the later stages of cardiac disease progression following 5/6 nephrectomy.

5. Limitations

We used a 5/6 nephrectomy to induce non-diabetic cardiorenal syndrome. However, three months after model induction, changes in cardiac function and structure were relatively mild. Extending the experimental duration may allow for the observation of a more significant cardioprotective effect of empagliflozin. In this study, left ventricular mass (LVM) was calculated based on echocardiographic parameters, but cardiac magnetic resonance imaging (cMRI) might provide a more accurate assessment of LVM. While single-nucleus RNA sequencing (snRNA-seq) is a precise and powerful tool for identifying multiple marker genes and clustering cell types, the sample size in this study was limited. Increasing the sample size and simultaneously using flow cytometry to count cardiomyocytes would help clarify the effect of empagliflozin on myocardial cell proliferation. In this study, we observed the impact of empagliflozin on immune cells, but since there was no model effect, we did not explore this further. Using snRNA-seq and qRT-PCR techniques, we found evidence that Empagliflozin exerts cardioprotective effects through the regulation of Fhl2 and Tbx20, but this does not fully explain the proposed mechanism. Additional animal experiments, such as cardiomyocyte-specific knockout of Fhl2 or overexpression of Tbx20, to assess the effects of Empagliflozin on cardiomyocyte hypertrophy and left ventricular mass gain, would further strengthen support for this hypothesis. Moreover, our conclusions are

based on an animal model exhibiting relatively mild cardiac injury. To further validate these findings, we are currently conducting studies using models with more severe myocardial damage, such as Angiotensin II-induced or Transverse Aortic Constriction (TAC)-induced cardiac hypertrophy.

6. Conclusion

This study provides compelling evidence that empagliflozin exerts a cardioprotective effect in a non-diabetic model of cardiorenal syndrome induced by 5/6 nephrectomy. Specifically, empagliflozin treatment led to a significant attenuation of left ventricular mass increase and a reduction in cardiomyocyte hypertrophy, effects that occurred independently of blood pressure changes. These structural improvements were accompanied by transcriptional changes in cardiomyocyte-specific genes, including upregulation of *Fhl2* and downregulation of *Tbx20*, pointing toward a direct, cell-intrinsic mechanism of action. Importantly, single-nuclei RNA sequencing revealed that these molecular changes were not associated with shifts in cell composition or proliferation, but rather reflected altered gene expression within cardiomyocytes.

The novelty of our findings lies in the identification of a mechanistic link between SGLT2 inhibition and cardiac structural remodeling through modulation of cardiomyocyte gene programs. While previous studies have demonstrated the cardiovascular benefits of empagliflozin in clinical populations, this study is among the first to provide cellular and transcriptional evidence for its direct myocardial effects in the absence of diabetes or overt heart failure.

Clinically, these results suggest that empagliflozin could be beneficial not only in the management of established heart failure or diabetic kidney disease, but also as a preventive therapy in early-stage cardiorenal syndrome—even in non-diabetic patients. The modulation of hypertrophy-related gene expression offers a potential explanation for the myocardial reverse remodeling observed in clinical trials such as EMPA-HEART and EMPA-KIDNEY, and supports broader use of SGLT2 inhibitors in high-risk populations.

Taken together, our data advance the mechanistic understanding of SGLT2 inhibitors and highlight their potential role in addressing the unmet need for early cardioprotection in chronic kidney disease. These findings lay the groundwork for future clinical studies investigating the use of empagliflozin in patients with early cardiac structural changes secondary to renal impairment.

CRediT authorship contribution statement

Denis Delić: Writing – review & editing, Visualization, Methodology, Formal analysis, Data curation, Conceptualization. **Nicolas Schommer:** Writing – review & editing, Methodology, Formal analysis. **Xin Chen:** Writing – review & editing, Writing – original draft, Validation, Project administration, Methodology, Investigation, Formal analysis, Data curation. **Christian T. Wohnhaas:** Writing – review & editing, Validation, Methodology, Formal analysis, Data curation. **Thomas Klein:** Writing – review & editing, Supervision, Methodology, Investigation, Conceptualization. **Ben He:** Writing – review & editing, Supervision, Methodology, Conceptualization. **Mohamed M.S. Gaballa:** Methodology, Formal analysis. **Bernhard K. Krämer:** Writing – review & editing, Supervision, Methodology, Conceptualization. **Zeyu Zhang:** Methodology, Investigation. **Christoph Reichetzeder:** Writing – review & editing, Supervision, Methodology, Formal analysis, Conceptualization. **Daniel Duerschmied:** Writing – review & editing, Supervision, Methodology, Conceptualization. **Yaochen Cao:** Methodology, Investigation, Formal analysis, Data curation. **Linghong Shen:** Writing – review & editing, Methodology, Formal analysis. **Berthold Hocher:** Writing – review & editing, Validation, Supervision, Methodology, Investigation, Formal analysis, Conceptualization.

Declaration of Competing Interest

The authors declare the following financial interests/personal relationships which may be considered as potential competing interests: Daniel Duerschmied reports a relationship with AOP Health, Bayer Healthcare, Boehringer Ingelheim, Sanofi, BMS, Pfizer, Boston Scientific, and Daiichi Sankyo that includes: speaking and lecture fees. Bernhard K. Kraemer reports a relationship with Astellas, Bayer, Boehringer Ingelheim, Chiesi, Riepharm, Pfizer, Sanofi, Servier and Vifor Pharma that includes: speaking and lecture fees. If there are other authors, they declare that they have no known competing financial interests or personal relationships that could have appeared to influence the work reported in this paper.

Acknowledgements

China Scholarship Council supported X.C. and Y.C.

Appendix A. Supporting information

Supplementary data associated with this article can be found in the online version at doi:10.1016/j.biopha.2025.118497.

Data availability

Data will be made available on request.

References

[1] C. Zoccali, P.B. Mark, P. Sarafidis, R. Agarwal, M. Adamczak, R. Bueno de Oliveira, Z.A. Massy, P. Kotanko, C.J. Ferro, C. Wanner, M. Burnier, R. Vanholder, F. Mallamaci, A. Wiecek, Diagnosis of cardiovascular disease in patients with chronic kidney disease, Nat. Rev. Nephrol. 19 (2023) 733–746, https://doi.org/10.1038/s41581-023-00747-4.

[2] S. Maqbool, S. Shafiq, S. Ali, M.E.U. Rehman, J. Malik, K.Y. Lee, Left ventricular hypertrophy (LVH) and left ventricular geometric patterns in patients with chronic kidney disease (CKD) stage 2-5 with preserved ejection fraction (EF): a systematic review to explore CKD Stage-wise LVH patterns, Curr. Probl. Cardiol. 48 (2023) 101590, https://doi.org/10.1016/j.cpcardiol.2023.101590.

[3] X. Wang, J.I. Shapiro, Evolving concepts in the pathogenesis of uraemic cardiomyopathy, Nat. Rev. Nephrol. 15 (2019) 159–175, https://doi.org/10.1038/s41581-018-0101-8.

[4] H.J.L. Heerspink, B.L. Neuen, L.A. Inker, Chronic kidney disease progression in heart failure: what we know, don't know, and where to next? JACC Heart Fail 12 (2024) 860–863, https://doi.org/10.1016/j.jchf.2024.02.028.

[5] J. Nespoux, V. Vallon, SGLT2 inhibition and kidney protection, Clin. Sci. (Lond) 132 (2018) 1329–1339, https://doi.org/10.1042/CS20171298.

[6] E.-K.C. Group, W.G. Herrington, N. Staplin, C. Wanner, J.B. Green, S.J. Hauske, J. R. Emberson, D. Preiss, P. Judge, K.J. Mayne, S.Y.A. Ng, E. Sammons, D. Zhu, M. Hill, W. Stevens, K. Wallendszus, S. Brenner, A.K. Cheung, Z.H. Liu, J. Li, L. S. Hooi, W. Liu, T. Kadowaki, M. Nangaku, A. Levin, D. Cherney, A.P. Maggioni, R. Pontremoli, R. Deo, S. Goto, X. Rossello, K.R. Tuttle, D. Steubl, M. Petrini, D. Massey, J. Eilbracht, M. Brueckmann, M.J. Landray, C. Baigent, R. Haynes, Empagliflozin in patients with chronic kidney disease, N. Engl. J. Med. (2022), https://doi.org/10.1056/NEJMoa2204233.

[7] H.J.L. Heerspink, B.V. Stefansson, R. Correa-Rotter, G.M. Chertow, T. Greene, F. F. Hou, J.F.E. Mann, J.J.V. McMurray, M. Lindberg, P. Rossing, C.D. Sjostrom, R. D. Toto, A.M. Langkilde, D.C. Wheeler, Committees D-CT, and investigators. Dapagliflozin in patients with chronic kidney disease, N. Engl. J. Med. 383 (2020) 1436–1446, https://doi.org/10.1056/NEJMoa2024816.

[8] D. Fitchett, S.E. Inzucchi, C.P. Cannon, D.K. McGuire, B.M. Scirica, O.E. Johansen, S. Sambevski, S. Kaspers, E. Pfarr, J.T. George, B. Zinman, Empagliflozin reduced mortality and hospitalization for heart failure across the spectrum of cardiovascular risk in the EMPA-REG OUTCOME trial, Circulation 139 (2019) 1384–1395, https://doi.org/10.1161/CIRCULATIONAHA.118.037778.

[9] M. Packer, S.D. Anker, J. Butler, G. Filippatos, S.J. Pocock, P. Carson, J. Januzzi, S. Verma, H. Tsutsui, M. Brueckmann, W. Jamal, K. Kimura, J. Schnee, C. Zeller, D. Cotton, E. Bocchi, M. Bohm, D.J. Choi, V. Chopra, E. Chuquiure, N. Giannetti, S. Janssens, J. Zhang, J.R. Gonzalez Juanatey, S. Kaul, H.P. Brunner-La Rocca, B. Merkely, S.J. Nicholls, S. Perrone, I. Pina, P. Ponikowski, N. Sattar, M. Senni, M. F. Seronde, J. Spinar, I. Squire, S. Taddei, C. Wanner, F. Zannad, And investigators EM-RT. Cardiovascular and renal outcomes with empagliflozin in heart failure, N. Engl. J. Med. 383 (2020) 1413–1424, https://doi.org/10.1056/NEJMoa2022190.

[10] S.D. Anker, J. Butler, G. Filippatos, J.P. Ferreira, E. Bocchi, M. Bohm, Rocca H. P. Brunner-La, D.J. Choi, V. Chopra, E. Chuquiure-Valenzuela, N. Giannetti, J. E. Gomez-Mesa, S. Janssens, J.L. Januzzi, J.R. Gonzalez-Juanatey, B. Merkely, S.

J. Nicholls, S.V. Perrone, I.L. Pina, P. Ponikowski, M. Senni, D. Sim, J. Spinar, I. Squire, S. Taddei, H. Tsutsui, S. Verma, D. Vinereanu, J. Zhang, P. Carson, C.S. P. Lam, N. Marx, C. Zeller, N. Sattar, W. Jamal, S. Schnaidt, J.M. Schnee, M. Brueckmann, S.J. Pocock, F. Zannad, M. Packer, And investigators EM-PT. Empagliflozin in heart failure with a preserved ejection fraction, N. Engl. J. Med. 385 (2021) 1451–1461, https://doi.org/10.1056/NEJMoa2107038.

[11] C.G. Santos-Gallego, A.P. Vargas-Delgado, J.A. Requena-Ibanez, A. Garcia-Ropero, D. Mancini, S. Pinney, F. Macaluso, S. Sartori, M. Roque, F. Sabatel-Perez, A. Rodriguez-Cordero, M.U. Zafar, I. Fergus, F. Atallah-Lajam, J.P. Contreras, C. Varley, P.R. Moreno, V.M. Abascal, A. Lala, R. Tamler, J. Sanz, V. Fuster, J. J. Badimon, And investigators E-T. Randomized trial of empagliflozin in nondiabetic patients with heart failure and reduced ejection fraction, J. Am. Coll. Cardiol. 77 (2021) 243–255, https://doi.org/10.1016/j.jacc.2020.11.008.

[12] J.A. Requena-Ibanez, C.G. Santos-Gallego, A. Rodriguez-Cordero, A.P. Vargas-Delgado, D. Mancini, S. Sartori, F. Atallah-Lajam, C. Giannarelli, F. Macaluso, A. Lala, J. Sanz, V. Fuster, J.J. Badimon, Mechanistic insights of empagliflozin in nondiabetic patients with HFrEF: from the EMPA-TROPISM study, JACC Heart Fail 9 (2021) 578–589, https://doi.org/10.1016/j.jchf.2021.04.014.

[13] A.J.M. Brown, S. Gandy, R. McCrimmon, J.G. Houston, A.D. Struthers, C.C. Lang, A randomized controlled trial of dapagliflozin on left ventricular hypertrophy in people with type two diabetes: the DAPA-LVH trial, Eur. Heart J. 41 (2020) 3421–3432, https://doi.org/10.1093/eurheartj/ehaa419.

[14] S. Verma, C.D. Mazer, A.T. Yan, T. Mason, V. Garg, H. Teoh, F. Zuo, A. Quan, M. E. Farkouh, D.H. Fitchett, S.G. Goodman, R.M. Goldenberg, M. Al-Omran, R. E. Gilbert, D.L. Bhatt, L.A. Leiter, P. Juni, B. Zinman, K.A. Connelly, Effect of empagliflozin on left ventricular mass in patients with type 2 diabetes mellitus and coronary artery disease: the EMPA-HEART CardioLink-6 randomized clinical trial, Circulation 140 (2019) 1693–1702, https://doi.org/10.1161/CIRCULATIONAHA.119.042375.

[15] R. Grempler, L. Thomas, M. Eckhardt, F. Himmelsbach, A. Sauer, D.E. Sharp, R. A. Bakker, M. Mark, T. Klein, P. Eickelmann, Empagliflozin, a novel selective sodium glucose cotransporter-2 (SGLT-2) inhibitor: characterisation and comparison with other SGLT-2 inhibitors, Diabetes Obes. Metab. 14 (2012) 83–90, https://doi.org/10.1111/j.1463-1326.2011.01517.x.

[16] P. Tauber, F. Sinha, R.S. Berger, W. Gronwald, K. Dettmer, M. Kuhn, M. Trum, L. S. Maier, S. Wagner, F. Schweda, Empagliflozin reduces renal hyperfiltration in response to uninephrectomy, but is not nephroprotective in UNx/DOCA/Salt mouse models, Front. Pharm. 12 (2021) 761855, https://doi.org/10.3389/fphar.2021.761855.

[17] A. Sarashina, K. Koiwai, L.J. Seman, N. Yamamura, A. Taniguchi, T. Negishi, S. Sesoko, H.J. Woerle, K.A. Dugi, Safety, tolerability, pharmacokinetics and pharmacodynamics of single doses of empagliflozin, a sodium glucose cotransporter 2 (SGLT2) inhibitor, in healthy Japanese subjects, Drug Metab. Pharm. 28 (2013) 213–219, https://doi.org/10.2133/dmpk.dmpk-12-rg-082.

[18] S. Zeng, D. Delic, C. Chu, Y. Xiong, T. Luo, X. Chen, M.M.S. Gaballa, Y. Xue, X. Chen, Y. Cao, A.A. Hasan, K. Stadermann, S. Frankenreiter, L. Yin, B.K. Kramer, T. Klein, B. Hocher, Antifibrotic effects of low dose SGLT2 inhibition with empagliflozin in comparison to ang II receptor blockade with telmisartan in 5/6 nephrectomised rats on high salt diet, Biomed. Pharm. 146 (2022) 112606, https://doi.org/10.1016/j.biopha.2021.112606.

[19] S.E. Litwin, S.E. Katz, E.O. Weinberg, B.H. Lorell, G.P. Aurigemma, P.S. Douglas, Serial echocardiographic-Doppler assessment of left ventricular geometry and function in rats with pressure-overload hypertrophy. Chronic angiotensin-converting enzyme inhibition attenuates the transition to heart failure, Circulation 91 (1995) 2642–2654, https://doi.org/10.1161/01.cir.91.10.2642.

[20] V. Stoyanova, N. Zhelev, E. Ghenev, M. Bosheva, Assessment of left ventricular structure and function in rats subjected to pressure-overload hypertrophy in time, Kardiol. Pol. 67 (2009) 27–34. ⟨https://www.ncbi.nlm.nih.gov/pubmed/19253187⟩. discussion 35.

[21] K. Kanasaki, S. Shi, M. Kanasaki, J. He, T. Nagai, Y. Nakamura, Y. Ishigaki, M. Kitada, S.P. Srivastava, D. Koya, Linagliptin-mediated DPP-4 inhibition ameliorates kidney fibrosis in streptozotocin-induced diabetic mice by inhibiting endothelial-to-mesenchymal transition in a therapeutic regimen, Diabetes 63 (2014) 2120–2131, https://doi.org/10.2337/db13-1029.

[22] E. Abdollahi, F. Keyhanfar, A.A. Delbandi, R. Falak, S.J. Hajimiresmaiel, M. Shafiei, Dapagliflozin exerts anti-inflammatory effects via inhibition of LPS-induced TLR-4 overexpression and NF-kappaB activation in human endothelial cells and differentiated macrophages, Eur. J. Pharm. 918 (2022) 174715, https://doi.org/10.1016/j.ejphar.2021.174715.

[23] Y.P. Lu, H.W. Wu, T. Zhu, X.T. Li, J. Zuo, A.A. Hasan, C. Reichetzeder, D. Delic, B. Yard, T. Klein, B.K. Kramer, Z.Y. Zhang, X.H. Wang, L.H. Yin, Y. Dai, Z.H. Zheng, B. Hocher, Empagliflozin reduces kidney fibrosis and improves kidney function by alternative macrophage activation in rats with 5/6-nephrectomy, Biomed. Pharm. 156 (2022) 113947, https://doi.org/10.1016/j.biopha.2022.113947.

[24] S.G. Lee, S.J. Lee, J.J. Lee, J.S. Kim, Lee OH, C.K. Kim, D. Kim, Y.H. Lee, J. Oh, S. Park, Jeon OH, S.J. Hong, C.M. Ahn, B.K. Kim, Y.G. Ko, D. Choi, M.K. Hong, Y. Jang, Anti-Inflammatory effect for atherosclerosis progression by Sodium-Glucose cotransporter 2 (SGLT-2) inhibitor in a normoglycemic rabbit model, Korean Circ. J. 50 (2020) 443–457, https://doi.org/10.4070/kcj.2019.0296.

[25] C.N. Koyani, I. Plastira, H. Sourij, S. Hallstrom, A. Schmidt, P.P. Rainer, H. Bugger, S. Frank, E. Malle, D. von Lewinski, Empagliflozin protects heart from inflammation and energy depletion via AMPK activation, Pharm. Res. 158 (2020) 104870, https://doi.org/10.1016/j.phrs.2020.104870.

[26] L. Liu, P. Kou, Q. Zeng, G. Pei, Y. Li, H. Liang, G. Xu, S. Chen, CD4+ T lymphocytes, especially Th2 cells, contribute to the progress of renal fibrosis, Am. J. Nephrol. 36 (2012) 386–396, https://doi.org/10.1159/000343283.

[27] Y. Dong, M. Yang, J. Zhang, X. Peng, J. Cheng, T. Cui, J. Du, Depletion of CD8+ T cells exacerbates CD4+ T cell-induced monocyte-to-fibroblast transition in renal fibrosis, J. Immunol. 196 (2016) 1874–1881, https://doi.org/10.4049/jimmunol.1501232.

[28] F. Soga, H. Tanaka, K. Tatsumi, Y. Mochizuki, H. Sano, H. Toki, K. Matsumoto, J. Shite, H. Takaoka, T. Doi, K.I. Hirata, Impact of dapagliflozin on left ventricular diastolic function of patients with type 2 diabetic mellitus with chronic heart failure, Cardiovasc. Diabetol. 17 (2018) 132, https://doi.org/10.1186/s12933-018-0775-z.

[29] S.R. Yurista, H.H.W. Sillje, S.U. Oberdorf-Maass, E.M. Schouten, M.G. Pavez Giani, J.L. Hillebrands, H. van Goor, D.J. van Veldhuisen, R.A. de Boer, B.D. Westenbrink, Sodium-glucose co-transporter 2 inhibition with empagliflozin improves cardiac function in non-diabetic rats with left ventricular dysfunction after myocardial infarction, Eur. J. Heart Fail 21 (2019) 862–873, https://doi.org/10.1002/ejhf.1473.

[30] C.G. Santos-Gallego, J.A. Requena-Ibanez, R. San Antonio, K. Ishikawa, S. Watanabe, B. Picatoste, E. Flores, A. Garcia-Ropero, J. Sanz, R.J. Hajjar, V. Fuster, J.J. Badimon, Empagliflozin ameliorates adverse left ventricular remodeling in nondiabetic heart failure by enhancing myocardial energetics, J. Am. Coll. Cardiol. 73 (2019) 1931–1944, https://doi.org/10.1016/j.jacc.2019.01.056.

[31] T. Takasu, S. Takakura, Effect of ipragliflozin, an SGLT2 inhibitor, on cardiac histopathological changes in a non-diabetic rat model of cardiomyopathy, Life Sci. 230 (2019) 19–27, https://doi.org/10.1016/j.lfs.2019.05.051.

[32] R.B. Devereux, B. Dahlof, E. Gerdts, K. Boman, M.S. Nieminen, V. Papademetriou, J. Rokkedal, K.E. Harris, J.M. Edelman, K. Wachtell, Regression of hypertensive left ventricular hypertrophy by losartan compared with atenolol: the losartan intervention for endpoint reduction in hypertension (LIFE) trial, Circulation 110 (2004) 1456–1462, https://doi.org/10.1161/01.CIR.0000141573.44737.5A.

[33] V. Palmieri, G. de Simone, M.J. Roman, J.E. Schwartz, T.G. Pickering, R. B. Devereux, Ambulatory blood pressure and metabolic abnormalities in hypertensive subjects with inappropriately high left ventricular mass, Hypertension 34 (1999) 1032–1040, https://doi.org/10.1161/01.hyp.34.5.1032.

[34] F. Paneni, S. Costantino, N. Hamdani, Regression of left ventricular hypertrophy with SGLT2 inhibitors, Eur. Heart J. 41 (2020) 3433–3436, https://doi.org/10.1093/eurheartj/ehaa530.

[35] P.H. Chu, P. Ruiz-Lozano, Q. Zhou, C. Cai, J. Chen, Expression patterns of FHL/SLIM family members suggest important functional roles in skeletal muscle and cardiovascular system, Mech. Dev. 95 (2000) 259–265, https://doi.org/10.1016/s0925-4773(00)00341-5.

[36] F.W. Friedrich, S. Reischmann, A. Schwalm, A. Unger, D. Ramanujam, J. Munch, O. J. Muller, C. Hengstenberg, E. Galve, P. Charron, W.A. Linke, S. Engelhardt, M. Patten, P. Richard, J. van der Velden, T. Eschenhagen, R. Isnard, L. Carrier, FHL2 expression and variants in hypertrophic cardiomyopathy, Basic Res. Cardiol. 109 (2014) 451, https://doi.org/10.1007/s00395-014-0451-8.

[37] R. Okamoto, Y. Li, K. Noma, Y. Hiroi, P.Y. Liu, M. Taniguchi, M. Ito, J.K. Liao, FHL2 prevents cardiac hypertrophy in mice with cardiac-specific deletion of ROCK2, FASEB J. 27 (2013) 1439–1449, https://doi.org/10.1096/fj.12-217018.

[38] B. Hojayev, B.A. Rothermel, T.G. Gillette, J.A. Hill, FHL2 binds calcineurin and represses pathological cardiac growth, Mol. Cell Biol. 32 (2012) 4025–4034, https://doi.org/10.1128/MCB.05948-11.

[39] N.H. Purcell, D. Darwis, O.F. Bueno, J.M. Muller, R. Schule, J.D. Molkentin, Extracellular signal-regulated kinase 2 interacts with and is negatively regulated by the LIM-only protein FHL2 in cardiomyocytes, Mol. Cell Biol. 24 (2004) 1081–1095, https://doi.org/10.1128/MCB.24.3.1081-1095.2004.

[40] F. Zhu, Q. Meng, Y. Yu, L. Shao, Z. Shen, Adult cardiomyocyte proliferation: a new insight for myocardial infarction therapy, J. Cardiovasc. Transl. Res. 14 (2021) 457–466, https://doi.org/10.1007/s12265-020-10067-8.

[41] M.K. Singh, V.M. Christoffels, J.M. Dias, M.O. Trowe, M. Petry, K. Schuster-Gossler, A. Burger, J. Ericson, A. Kispert, Tbx20 is essential for cardiac chamber differentiation and repression of Tbx2, Development 132 (2005) 2697–2707, https://doi.org/10.1242/dev.01854.

[42] T. Shen, I. Aneas, N. Sakabe, R.J. Dirschinger, G. Wang, S. Smemo, J.M. Westlund, H. Cheng, N. Dalton, Y. Gu, C.J. Boogerd, C.L. Cai, K. Peterson, J. Chen, M. A. Nobrega, S.M. Evans, Tbx20 regulates a genetic program essential to adult mouse cardiomyocyte function, J. Clin. Invest. 121 (2011) 4640–4654, https://doi.org/10.1172/JCI59472.

[43] L. Qian, B. Mohapatra, T. Akasaka, J. Liu, K. Ocorr, J.A. Towbin, R. Bodmer, Transcription factor neuromancer/TBX20 is required for cardiac function in drosophila with implications for human heart disease, Proc. Natl. Acad. Sci. USA 105 (2008) 19833–19838, https://doi.org/10.1073/pnas.0808705105.

[44] N.J. Sakabe, I. Aneas, T. Shen, L. Shokri, S.Y. Park, M.L. Bulyk, S.M. Evans, M. A. Nobrega, Dual transcriptional activator and repressor roles of TBX20 regulate adult cardiac structure and function, Hum. Mol. Genet. 21 (2012) 2194–2204, https://doi.org/10.1093/hmg/dds034.

[45] F.L. Xiang, M. Guo, K.E. Yutzey, Overexpression of Tbx20 in adult cardiomyocytes promotes proliferation and improves cardiac function after myocardial infarction, Circulation 133 (2016) 1081–1092, https://doi.org/10.1161/CIRCULATIONAHA.115.019357.

[46] S. Das, A. Mondal, C. Dey, S. Chakraborty, R. Bhowmik, S. Karmakar, A. Sengupta, ER stress induces upregulation of transcription factor Tbx20 and downstream Bmp2 signaling to promote cardiomyocyte survival, J. Biol. Chem. 299 (2023) 103031, https://doi.org/10.1016/j.jbc.2023.103031.

[47] R.R. Vanderpool, A. Gorelova, Y. Ma, M. Alhamaydeh, J. Baust, S. Shiva, S. P. Tofovic, J. Hu, S.M. Nouraie, M.T. Gladwin, M. Sharifi-Sanjani, I. Al Ghouleh, Reversal of right ventricular hypertrophy and dysfunction by prostacyclin in a rat

model of severe pulmonary arterial hypertension, Int. J. Mol. Sci. 23 (2022), https://doi.org/10.3390/ijms23105426.

[48] X. Chen, C.F. Hocher, L. Shen, B.K. Kramer, B. Hocher, Reno- and cardioprotective molecular mechanisms of SGLT2 inhibitors beyond glycemic control: from bedside to bench, Am. J. Physiol. Cell Physiol. 325 (2023) C661–C681, https://doi.org/10.1152/ajpcell.00177.2023.

[49] H. Liu, P. Wei, W. Fu, C. Xia, Y. Li, K. Tian, Y. Li, D. Cheng, J. Sun, Y. Xu, M. Lu, B. Xu, Y. Zhang, R. Wang, W. Wang, B. Xu, E. Liu, S. Zhao, Dapagliflozin ameliorates the formation and progression of experimental abdominal aortic aneurysms by reducing aortic inflammation in mice, Oxid. Med. Cell Longev. 2022 (2022) 8502059, https://doi.org/10.1155/2022/8502059.